Available online at www.sciencedirect.com
SCIENCE DIRECT
Journal of the European Ceramic Society 26 (2006) 559–563
www.elsevier.com/locate/jeurceramsoc

Control of crystalline texture in polycrystalline TiO_2 (Anatase) by electrophoretic deposition in a strong magnetic field

Tetsuo Uchikoshi [a,*], Tohru S. Suzuki [a], Shuji Iimura [b], Fengqiu Tang [a], Yoshio Sakka [a]

[a] *National Institute for Materials Science, 1-2-1 Sengen, Tsukuba, Ibaraki 305-0047, Japan*
[b] *Ibaraki Industrial Technology Institute, Ibaraki-town, Ibaraki 311-3195, Japan*

Available online 18 August 2005

Abstract

Crystalline oriented titania (anatase) thick films have been fabricated by electrophoretic deposition in a strong 12 T magnetic field. Anatase particles in an aqueous suspension are rotated due to their magnetic anisotropy and then deposited on a substrate in a dc electric field. The angle between the directions of the magnetic and electric fields φ_{B-E} is fixed at specified angles (φ_{B-E} = 0, 30, 60 and 90°) during the deposition to control the dominant crystalline orientation of the deposits. The crystalline orientation characterized by the X-ray diffraction for the anatase films proves the orientation dependence of anatase upon the φ_{B-E} angle during the EPD. The crystalline orientation of the anatase films can be controlled by varying the angle of $\boldsymbol{E}$ versus $\boldsymbol{B}$.

Keywords: TiO_2; Suspension; Functional applications; Microstructure-prefiring; Electrophoretic deposition

1. Introduction

Titanium dioxide, TiO_2, has been extensively studied for its unique physical and chemical properties, such as high refractive index, excellent optical transmittance in the visible and near-infrared region, high dielectric constant, and photocatalysis for water cleavage. Titania has three crystallographic polymorphs, i.e., rutile, anatase and brookite, composed of Ti ions having octahedral coordination. Though rutile is the most thermodynamically stable phase, anatase shows advantages in photocatalysis and energy conversion. Besides, it has been reported for anatase that there is an orientation dependence of the reaction activity. For example, water reduction and photo oxidation take place at more negative potentials for the anatase (0 0 1) surface than for the anatase (1 0 1) surface.[1] Orienting anatase nanocrystals with (0 0 1) preferred growth may improve the charge conversion efficiency of photocatalysis and dye-sensitized nanocrystalline cells.[2] Due to the difficulty in obtaining a natural anatase single crystal, studies on the orientation dependence of the physical and chemical properties of anatase have been limited.[3,4]

In general, the artificial crystal growth of anatase is not easy since anatase is a low temperature-stable phase and easily transforms to rutile above ∼700 °C. Single-crystalline anatase has been prepared by a chemical transport reaction.[5,6] Appropriate choice of substrate material has also enabled us to grow anatase with preferred orientations. For example (0 0 1) oriented anatase films have been prepared on $LaAlO_3$ (0 0 1) and $SrTiO_3$ (0 0 1) single crystals by chemical vapor deposition (CVD),[7] pulsed laser deposition,[8] molecular beam epitaxy (MBE)[9] and laser MBE[10,11] since the lattice mismatch of *a*-axis constants between $LaAlO_3$ or $SrTiO_3$ and TiO_2 is very small. However, these methods are not practicable for fabricating oriented titania onto other various substrate materials.

Recently, we developed a promising processing technique to fabricate a polycrystalline ceramic thick film with preferred crystalline orientation using commercial powder by electrophoretic deposition (EPD)[12–14] in a strong magnetic field. A schematic illustration of the concept has been shown in previous papers.[15–18] Ceramic particles dispersed in a solvent are rotated due to their magnetic anisotropy and then

* Corresponding author. Tel.: +81 29 859 2460; fax: +81 29 859 2401.
E-mail address: uchikoshi.tetsuo@nims.go.jp (T. Uchikoshi).

0955-2219/$ – see front matter © 2005 Elsevier Ltd. All rights reserved.
doi:10.1016/j.jeurceramsoc.2005.06.044

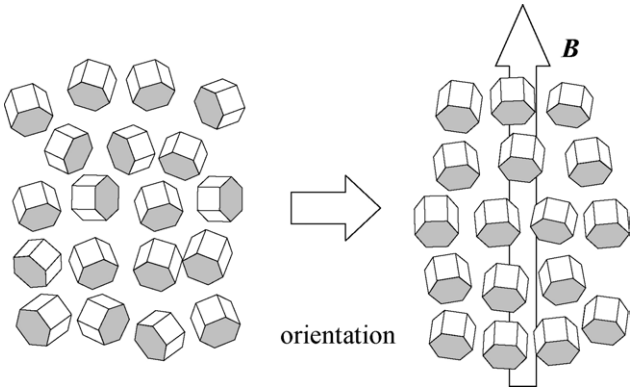

Fig. 1. Schematic illustration of the orientation of single crystalline particles in a magnetic field.

deposited on a substrate in a dc electric field. The fundamental concept is as follows.

Many materials in asymmetric (non-cubic) crystalline structures have anisotropic magnetic susceptibilities, $\Delta\chi = \chi_{\parallel} - \chi_{\perp}$, associated with their crystal structures, where $\chi_{\parallel}$ and $\chi_{\perp}$ are the susceptibilities parallel and perpendicular to the magnetic principal axis, respectively. When a single crystal of these materials is placed in a magnetic field, the crystal is rotated and the crystallographic axis of high χ is aligned in the direction of the magnetic field. A schematic illustration of the rotation of particles in a magnetic field is shown in Fig. 1. The driving force of the magnetic alignment is the energy of the crystal anisotropy and is given as $\Delta E = \Delta\chi VB^2/2\mu_0$, where V is the volume of the material, B the applied magnetic field, and μ_0 is the permeability in a vacuum.[19] Generally, the magnetic susceptibilities of feeble magnetic materials ($|\chi| = 10^{-3}$ to 10^{-6}) are quite low in comparison with those of ferromagnetic materials ($|\chi| = 10^{2}$–10^{4}) and the ΔE of feeble magnetic materials is much lower than the energy of thermal motion, kT, in a conventional magnetic field generated by a permanent magnet ($B = \sim 10^{-1}$ T). However, the magnetization force acting on feeble magnetic materials can be higher than kT at room temperature under a strong magnetic field as high as ~10 T.[17]

Anatase has a tetragonal crystalline structure and is very likely to be aligned with the direction of the magnetic field at ~10 T. We demonstrate in this paper that anatase thick films with a preferred crystalline orientation are fabricated by EPD in a superconducting magnet.

2. Experimental

Spherical anatase particles (Nanotek TiO_2, 80% anatase, average particle size of 30 nm, high purity of 99.95%) were used in this study. The transmission electron microscopic (TEM) photograph and X-ray diffraction (XRD) pattern of the as-received powder are shown in Figs. 2 and 3, respectively. The powder was dispersed in distilled water at pH 5.5 by ultrasounds, and then a deflocculated titania suspension

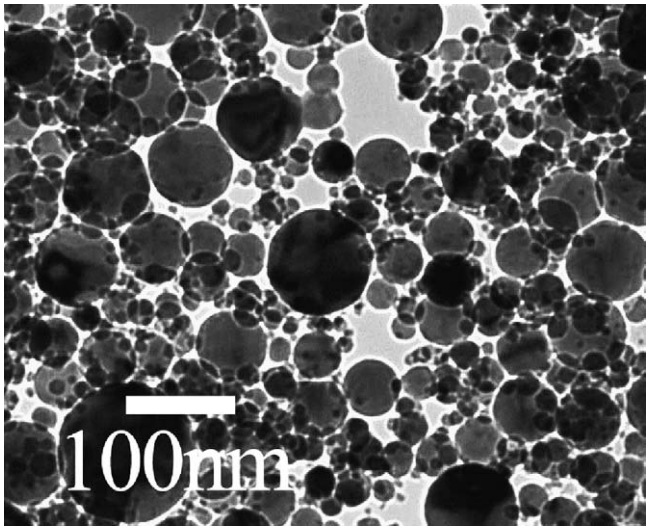

Fig. 2. TEM photograph of as-received titania powder.

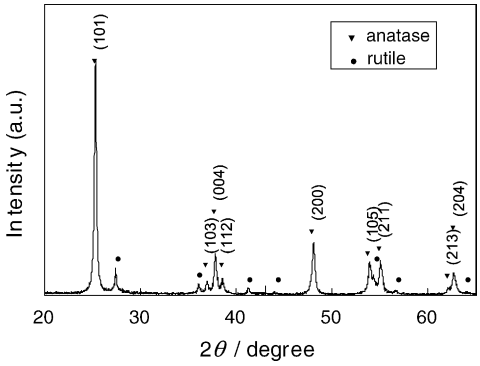

Fig. 3. XRD pattern of as-received titania powder.

with a 5 vol.% solid content was prepared. Polyethylenimine (PEI) was added to improve the stability of the suspension.[20] The zeta-potentials of the anatase powder with and without PEI modification are shown in Fig. 4. The suspension was placed in the center of the magnetic field of a superconducting magnet (Japan Superconductor Tech. Inc., JMTD-12T100NC5) and then a strong magnetic field was applied to the suspension to rotate each particle. The magnetic field

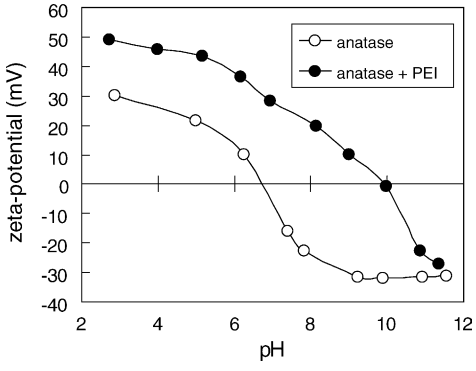

Fig. 4. Zeta-potentials of anatase powder with and without PEI modification.

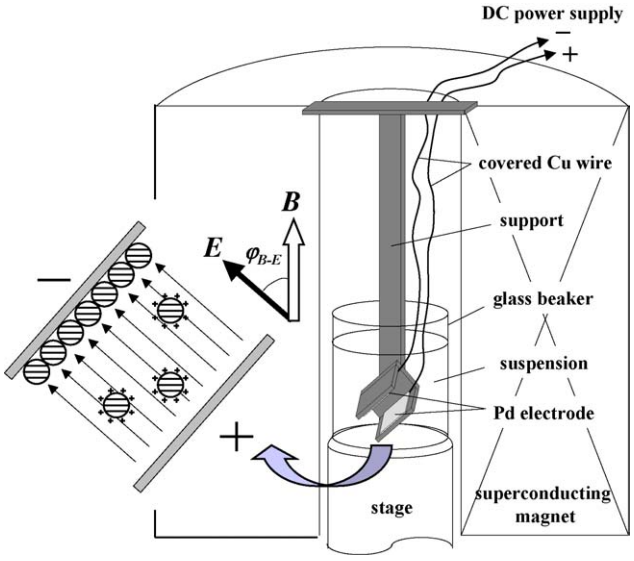

Fig. 5. Schematic illustration of the apparatus for EPD in a superconducting magnet.

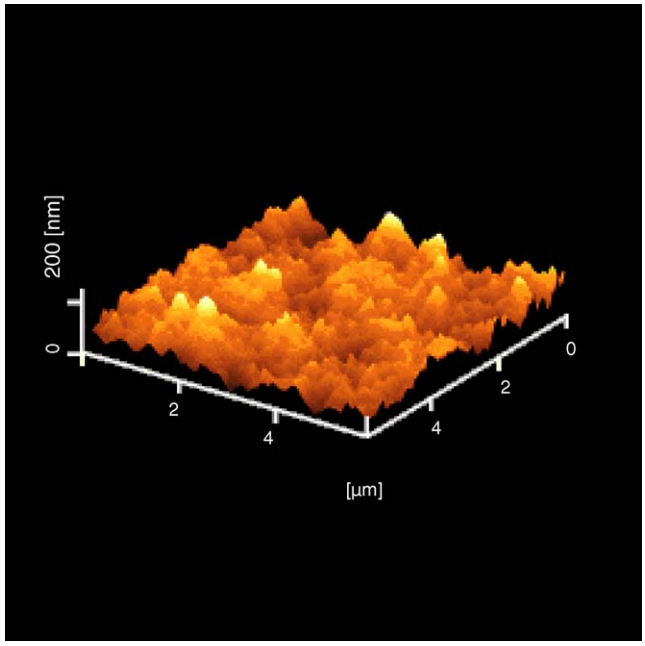

Fig. 6. AFM photograph of the deposit surface.

was maintained in the suspension during the EPD at a constant current of 2.7 mA/cm^2. A schematic illustration of the apparatus is shown in Fig. 5. The magnetic field fixes the orientation of each particle; the *c*-axis of the anatase is aligned parallel to ***B*** in this case.[21] When an electrical field is then applied to the oriented particles, they move along with the electric field lines while retaining their orientation relative to the magnetic field, and then deposit on a substrate. A palladium sheet was used as the cathodic substrate to absorb the hydrogen produced by electrolysis of the solvent.[22] The direction of the electric field ***E*** relative to the magnetic field ***B*** was altered ($\varphi_{B-E} = 0$, 30, 60 and 90°) in order to control the preferred orientation of the anatase deposits. After the deposition, the deposits were removed from the magnetic field and dried at room temperature. The surface roughness of the deposit was observed by an atomic force microscope (AFM). The XRD analysis was carried out to investigate the crystalline orientation of the specimens. The green density of the deposit was measured for a thick deposit separated from a substrate by Archimedes' method.

3. Results and discussion

An AFM photograph of the deposit surface is shown in Fig. 6. The surface of the deposit is considerably flat and smooth. The green density of the deposit was 61.2% of the theoretical density. The use of a palladium substrate effectively suppressed the hydrogen bubble formation at the cathode and dense, bubble-free deposits were obtained.

Fig. 7 shows the XRD patterns of the anatase deposited at 12 T. The direction of the electric field ***E*** was fixed parallel to that of the magnetic field ***B*** ($\varphi_{B-E} = 0°$) so as not to be affected by the Lorentz force during the deposition. The diffraction peak of the (0 0 4) plane is strong for the top of the deposit, while the diffraction peak of the (2 0 0) plane is strong for the side of the deposit. The figure shows that thick anatase films with a preferred crystalline orientation are fabricated by this technique.

Fig. 8 shows the XRD patterns of the anatase deposited at 0 T (external to the magnetic field). No difference is observed between the XRD patterns of the top and the side planes of the deposit. The diffraction patterns in Fig. 8 are also similar to that of the as-received powder in Fig. 3. It is obvious that the specimen prepared without the influence of the magnetic field has a randomly oriented structure.

Fig. 9 shows the variation in the XRD patterns of the top of the deposits with the angle between the directions of ***B*** and ***E*** (φ_{B-E}). The angles noted next to the *hkl* indices are the interplanar angles ϕ_{hkl} between the ($h\,k\,l$) planes and the (0 0 *l*)

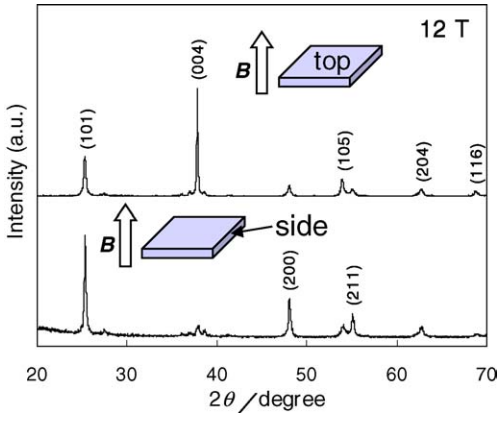

Fig. 7. XRD patterns of the top and side planes of the anatase deposited at 12 T. The direction of the electric field ***E*** was fixed parallel to that of the magnetic field ***B*** ($\varphi_{B-E} = 0°$).

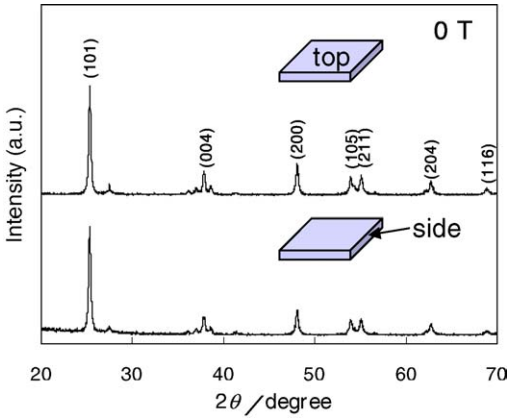

Fig. 8. XRD patterns of the top and side planes of the anatase deposited at 0 T.

basal plane calculated for a tetragonal unit cell of anatase. From the XRD pattern in Fig. 9, the intensity of the diffraction peak of the (0 0 4) plane ($\phi_{004} = 0^\circ$) is very strong in comparison with the XRD data in Fig. 3 when $\boldsymbol{E}$ is parallel to $\boldsymbol{B}$ ($\varphi_{B-E} = 0^\circ$). In contrast, the diffraction peaks of the planes at high interplanar angles such as (1 0 1) ($\phi_{101} = 67.5^\circ$), (2 0 0) ($\phi_{200} = 90^\circ$) and (2 1 1) ($\phi_{211} = 79.5^\circ$) are relatively weak. The XRD data show that the anatase film prepared at $\varphi_{B-E} = 0^\circ$ has a (0 0 1) preferred orientation. When φ_{B-E} is changed to 30°, the diffraction peak of the (0 0 4) plane becomes weak and the peak of (1 0 5) ($\phi_{105} = 25.8^\circ$) becomes relatively strong. The peak of the (1 0 1) ($\phi_{101} = 67.5^\circ$) plane also becomes stronger. When φ_{B-E} is changed to 60°, the diffraction peak of the (0 0 4) becomes much weaker and the peak of the (1 0 1) plane becomes the strongest one. This anatase film has a (1 0 1) preferred orientation. Finally, when $\boldsymbol{E}$ is perpendicular to $\boldsymbol{B}$ ($\varphi_{B-E} = 90^\circ$), the diffraction peak of the (2 0 0) plane becomes much strong. The peak of the (2 1 1) ($\phi_{211} = 79.5^\circ$) plane is also relatively stronger. The XRD data show that the dominant crystal orientation of the deposit is controllable by varying the angle of $\boldsymbol{E}$ versus $\boldsymbol{B}$. When $\boldsymbol{E} \times \boldsymbol{B} \neq 0$, the particles should be affected by the Lorentz force. It is probable that the Lorentz force causes stirring of the suspension and disturbs the orientation of each particle during deposition. Therefore, the orientation at $\varphi_{B-E} = 30$, 60 and 90° was inferior to that at $\varphi_{B-E} = 0^\circ$. The following thermal treatment at 650 °C somewhat improved the orientation of anatase, but the heating at 700 °C spoiled the orientation due to the phase transformation from anatase to rutile.

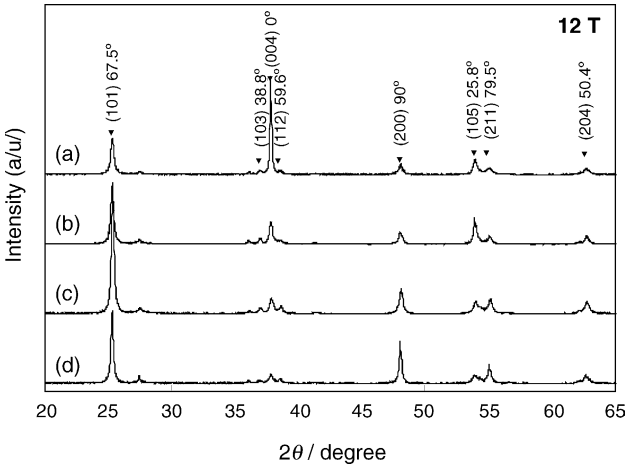

Fig. 9. XRD patterns of the top surfaces of as-deposited titania films and their $\boldsymbol{B}$–$\boldsymbol{E}$ angle (φ_{B-E}) dependence: (a) $\varphi_{B-E} = 0^\circ$, (b) $\varphi_{B-E} = 30^\circ$, and (c) $\varphi_{B-E} = 60^\circ$ and (d) $\varphi_{B-E} = 90^\circ$. The interplanar angles ϕ_{hkl} between the planes ($h\,k\,l$) and the basal plane (0 0 l) of a tetragonal unit cell of titania are also shown in this figure.

4. Conclusions

The magnetic field fixes the orientation of each particle; the c-axis of anatase is aligned parallel to $\boldsymbol{B}$ in the suspension. When an electrical field is then applied to the oriented particles, they move along the electric field lines while retaining their orientation against the magnetic field lines, and then deposit on the substrate. By varying the angle between the vectors $\boldsymbol{E}$ and $\boldsymbol{B}$, the crystalline orientation of the deposits can be controlled.

Acknowledgments

The authors wish to thank Dr. Naoto Shirahata of the National Institute for Materials Science for his AFM observations. This research was partially supported by the Budget for Nuclear Research of the Ministry of Education, Culture, Sports, Science and Technology (MEXT) and a grant-in-aid for Scientific Research (no. 15560593) from the MEXT.

References

1. Hengerer, R., Kavan, L., Krtil, P. and Grätzel, M., Orientation dependence of charge-transfer processes on TiO_2 (Anatase) single crystals. *J. Electrochem. Soc.*, 2000, **147**, 1467–1472.
2. Deng, H., Zhang, H. and Lu, Z., Dye-sensitized anatase titanium dioxide nanocrystalline with (0 0 1) preferred orientation induced by Langmuir-Bloggett monolayer. *Chem. Phys. Lett.*, 2002, **363**, 509–514.
3. Hebenstreit, W., Ruzycki, N., Herman, G. S., Gao, Y. and Diebold, U., Scanning tunneling microscopy investigation of the TiO_2 anatase (1 0 1) surface. *Phys. Rev. B*, 2000, **62**, R16334–R16336.
4. Ruzycki, N., Herman, G. S., Boatner, L. A. and Diebold, U., Scanning tunneling microscopy study of the anatase (1 0 0) surface. *Surf. Sci.*, 2003, **529**, L239–L244.
5. Berger, H., Tang, H. and Lévy, F., Growth and Raman spectroscopic characterization of TiO_2 anatase single crystals. *J. Cryst. Growth*, 1993, **130**, 108–112.
6. Kavan, L., Grätzel, M., Gilbert, S. E., Klements, C. and Scheel, H. J., Electrochemical and photoelectrochemical investigation of single-crystal Anatase. *J. Am. Chem. Soc.*, 1996, **118**, 6716–6723.
7. Chen, S., Mason, M. G., Gysling, H. J., Paz-Pujalt, G. R., Blanton, T. N., Castro, T. *et al.*, Ultrahigh vacuum metalogranic chemical vapor

deposition growth and in situ characterization of epitaxial TiO_2 films. *J. Vac. Sci. Tech.*, 1993, **A 11**, 2419–2429.
8. Sumita, T., Yamaki, T., Yamamoto, S. and Miyashita, A., Photo-induced surface change separation of highly oriented TiO_2 anatase and rutile thin films. *Appl. Surf. Sci.*, 2000, **200**, 21–26.
9. Sugimura, W., Yamazaki, A., Shigetani, H., Tanaka, J. and Mitsuhashi, T., *Jpn. J. Appl. Phys.*, 1997, **36**, 7358–7359.
10. Murakami, M., Matsumoto, Y., Nakajima, K., Makino, T., Segawa, Y., Chikyow, T. *et al.*, Anatase TiO_2 thin films grown on lattice-matched $LaAlO_3$ substrate by laser molecular-beam epitaxy. *Appl. Phys. Lett.*, 2001, **78**, 2664–2666.
11. Ong, C. K. and Wang, S. J., In situ RHEED monitor of the growth of epitaxial anatase TiO_2 thin films. *Appl. Surf. Sci.*, 2001, **185**, 47–51.
12. Sarkar, P. and Nicholson, P. S., Electrophoretic deposition (EPD): mechanisms, kinetics, and application to ceramics. *J. Am. Ceram. Soc.*, 1996, **79**, 1987–2002.
13. Van der Biest, O. O. and Vandeperre, L. J., Electrophoretic deposition of materials. *Annu. Rev. Mater. Sci.*, 1999, **29**, 327–352.
14. Boccaccini, A. R. and Zhitomirsky, I., Application of electrophoretic deposition techniques in ceramic processing. *Curr. Opin. Solid State Mater. Sci.*, 2002, **6**, 251–260.
15. Uchikoshi, T., Suzuki, T. S., Okuyama, H. and Sakka, Y., Electrophoretic deposition of α-alumina particles in a strong magnetic field. *J. Mater. Res.*, 2003, **18**, 254–256.
16. Uchikoshi, T., Suzuki, T. S., Okuyama, H. and Sakka, Y., Fabrication of textured alumina by electrophoretic deposition in a strong magnetic field. *J. Mater. Sci.*, 2004, **39**, 861–865.
17. Uchikoshi, T., Suzuki, T. S., Okuyama, H. and Sakka, Y., Electrophoretic deposition of alumina suspension in a strong magnetic field. *J. Eur. Ceram. Soc.*, 2004, **24**, 225–229.
18. Uchikoshi, T., Suzuki, T. S., Okuyama, H. and Sakka, Y., Control of crystalline texture in polycrystalline alumina ceramics by electrophoretic deposition in a strong magnetic field. *J. Mater. Res.*, 2004, **19**, 1487–1491.
19. de Rango, P., Lees, M., Lejay, P., Sulpice, A., Tournier, R., Ingold, M. *et al.*, Texturing of magnetic materials at high temperature by solidification in a magnetic field. *Nature*, 1991, **349**, 770–772.
20. Tang, F., Ozawa, K., Uchikoshi, T. and Sakka, Y., Dispersion of titania aqueous suspensions with polyethylenimine polyelectrolyte. *J. Ceram. Soc. Jpn.*, 2004, **112**(Suppl.), S950–S953.
21. Suzuki, T. S. and Sakka, Y., Fabrication of textured titania by slip casting in a high magnetic field followed by heating. *Jpn. J. Appl. Phys.*, 2002, **41**, L1272–L1274.
22. Uchikoshi, T., Ozawa, K., Hatton, B. D. and Sakka, Y., Dense, bubble-free ceramic deposits from aqueous suspensions by electrophoretic deposition. *J. Mater. Res.*, 2001, **16**, 321–324.